

**CHEMISTRY AND TECHNOLOGY OF MEDICINAL COMPOUNDS  
AND BIOLOGICALLY ACTIVE SUBSTANCES**

**ХИМИЯ И ТЕХНОЛОГИЯ ЛЕКАРСТВЕННЫХ ПРЕПАРАТОВ  
И БИОЛОГИЧЕСКИ АКТИВНЫХ СОЕДИНЕНИЙ**

ISSN 2686-7575 (Online)

<https://doi.org/10.32362/2410-6593-2021-16-5-414-425>



УДК 541.64+57.083.3+535.371+616-097

RESEARCH ARTICLE

**Characterization of iron-doped crystalline silicon nanoparticles  
and their modification with citrate anions for *in vivo* applications**

**Kirill I. Rozhkov<sup>1,\*</sup>, Elena Y. Yagudaeva<sup>2</sup>, Svetlana V. Sizova<sup>2</sup>, Michael A. Lazov<sup>1</sup>,  
Evgeniya V. Smirnova<sup>2</sup>, Vitaliy P. Zubov<sup>1,2</sup>, Anatoliy A. Ischenko<sup>1</sup>**

<sup>1</sup>MIREA – Russian Technological University (M.V. Lomonosov Institute of Fine Chemical Technologies),  
Moscow, 119571 Russia

<sup>2</sup>Shemyakin and Ovchinnikov Institute of Bioorganic Chemistry, Russian Academy of Sciences,  
Moscow, 117997 Russia

\*Corresponding author, e-mail: rokirill58@mail.ru

**Abstract**

**Objectives.** This paper presents data on the development and study of the structural properties of iron-doped crystalline silicon (nc-Si/SiO<sub>x</sub>/Fe) nanoparticles obtained using the plasma-chemical method for application in magnetic resonance imaging diagnostics and treatment of oncological diseases. This work aimed to use a variety of analytical methods to study the structural properties of nc-Si/SiO<sub>x</sub>/Fe and their colloidal stabilization with citrate anions for *in vivo* applications.

**Methods.** Silicon nanoparticles obtained via the plasma-chemical synthesis method were characterized by laser spark emission spectroscopy, atomic emission spectroscopy, Fourier-transform infrared spectroscopy, and X-ray photoelectron spectroscopy. The hydrodynamic diameter of the nanoparticles was estimated using dynamic light scattering. The toxicity of the nanoparticles was investigated using a colorimetric MTT test for the cell metabolic activity. Elemental iron with different Fe/Si atomic ratios was added to the feedstock during loading.

**Results.** The particles were shown to have a large silicon core covered by a relatively thin layer of intermediate oxides (interface) and an amorphous oxide shell, which is silicon oxide with different oxidation states SiO<sub>x</sub> (0 ≤ x ≤ 2). The samples had an iron content of 0.8–1.8 at %. Colloidal solutions of the nanoparticles stabilized by citrate anions were obtained and characterized. According to the analysis of the cytotoxicity of the modified nanosilicon particles using monoclonal K562 human erythroleukemia cells, no toxicity was found for cells in culture at particle concentrations of up to 5 μg/mL.

**Conclusions.** Since the obtained modified particles are nontoxic, they can be used in *in vivo* theranostic applications.

**Keywords:** silicon nanoparticles, iron, magnetic resonance imaging, citrate anions, X-ray photoelectron spectroscopy, Fourier-transform infrared spectroscopy, cytotoxicity

**For citation:** Rozhkov K.I., Yagudaeva E.Y., Sizova S.V., Lazov M.A., Smirnova E.V., Zubov V.P., Ischenko A.A. Characterization of iron-doped crystalline silicon nanoparticles and their modification with citrate anions for *in vivo* applications. *Tonk. Khim. Tekhnol. = Fine Chem. Technol.* 2021;16(5):414–425 (Russ., Eng.). <https://doi.org/10.32362/2410-6593-2021-16-5-414-425>

## НАУЧНАЯ СТАТЬЯ

# Характеризация наночастиц кристаллического кремния, легированного железом, и их модификация цитрат-анионами для использования *in vivo*

К.И. Рожков<sup>1,@</sup>, Е.Ю. Ягудаева<sup>2</sup>, С.В. Сизова<sup>2</sup>, М.А. Лазов<sup>1</sup>, Е.В. Смирнова<sup>2</sup>, В.П. Зубов<sup>1,2</sup>, А.А. Ищенко<sup>1</sup>

<sup>1</sup>МИРЭА – Российский технологический университет (Институт тонких химических технологий им. М.В. Ломоносова), Москва, 119571 Россия

<sup>2</sup>Институт биоорганической химии им. академиков М.М. Шемякина и Ю.А. Овчинникова Российской академии наук, Москва, 117997 Россия

@ Автор для переписки, e-mail: [rokirill58@mail.ru](mailto:rokirill58@mail.ru)

### Аннотация

**Цели.** В работе приводятся данные по разработке и изучению структурных свойств полученных плазмохимическим методом наночастиц кремния  $nc\text{-Si}/\text{SiO}_x/\text{Fe}$ , легированных железом. Цель работы – исследование свойств наночастиц кремния, легированных железом, комплексом аналитических методов и их стабилизация цитрат-анионами для применения в диагностике методом магнитно-резонансной томографии и лечении онкологических заболеваний.

**Методы.** Наночастицы кремния, полученные плазмохимическим методом синтеза, были охарактеризованы лазерно-искровым эмиссионным методом, методом атомной эмиссионной спектроскопии, Фурье-ИК-спектроскопией, рентгеновской фотоэлектронной спектроскопией. Гидродинамический диаметр наночастиц оценивали методом динамического светорассеяния. Исследование токсичности наночастиц проводили с помощью колориметрического МТТ теста на метаболическую активность клеток. В исходное сырье при загрузке добавляли элементарное железо с разным атомным соотношением Fe/Si.

**Результаты.** Было показано, что частица имеет кремниевое ядро с аморфной оксидной оболочкой, представляющей собой оксиды кремния с разной степенью окисления  $\text{SiO}_x$  ( $0 \leq x \leq 2$ ). Содержание железа в образцах составило от 0.8 до 1.8 ат. %. Были получены и охарактеризованы коллоидные растворы наночастиц, стабилизированные цитрат-анионами. Анализ цитотоксичности модифицированных частиц нанокремния с использованием моноклонизированных клеток эритролейкоза человека K562 показал отсутствие токсичности для клеток в культуре при концентрации частиц до 5 мкг/мл.

**Выводы.** Полученные модифицированные частицы не обладают токсичностью, поэтому их можно рекомендовать для использования в *in vivo* приложениях для терапии.

**Ключевые слова:** наночастицы кремния, железа, цитрат-анионы, рентгеновская фотоэлектронная спектроскопия, Фурье-инфракрасная спектроскопия, цитотоксичность

**Для цитирования:** Рожков К.И., Ягудаева Е.Ю, Сизова С.В., Лазов М.А., Смирнова Е.В., Зубов В.П., Ищенко А.А. Характеризация наночастиц кристаллического кремния, легированного железом, и их модификация цитрат-анионами для использования *in vivo*. *Тонкие химические технологии*. 2021;16(5):414–425. <https://doi.org/10.32362/2410-6593-2021-16-5-414-425>

## INTRODUCTION

Various nanoparticles, such as paramagnetic complexes of gadolinium(III), iron(III), and manganese(III), are currently used in magnetic resonance imaging (MRI). Despite the high efficiency of contrasting properties and widespread use in medicine, these complexes can cause allergic reactions and nephrogenic systemic fibrosis and accumulate in the brain for a long time [1, 2]. The use of superparamagnetic iron oxide ( $\text{Fe}_2\text{O}_3$ ) nanoparticles is unsafe for living organisms because their high magnetic moment causes significant disturbances in the magnetic field in the body [3]. Therefore, the search for new contrast agents is still ongoing.

Many researchers are interested in using nanosized silicon particles and their composites for *in vivo* applications because they do not exhibit toxic properties and are biodegradable and biocompatible [4]. Silicon is one of the most important trace elements involved in the connective tissue repair mechanisms of the body [5]. Silicon nanoparticles in living organisms undergo biodegradation, forming orthosilicic acid, which is then easily removed [6].

The superparamagnetic properties of porous silicon dioxide nanoparticles with embedded magnetic nanoparticles have been demonstrated to be promising for magnetically targeted delivery of therapeutic molecules and have significant clinical application potential [7]. Hollow silicon nanospheres doped

with  $\text{Fe}^{3+}$  ions, of which the surface is modified with silane-polyethylene glycol (silane-PEG-COOH), can be used as a low-cytotoxic and dual-mode ultrasonic and magnetic resonance (US–MR) specific imager in biopharmaceutical applications and clinical diagnosis and treatment [8]. Magnetic particles based on  $\text{Fe}_3\text{O}_4$  with a surface stabilized by silicon dioxide and citrate ions are promising for the creation of drug delivery vehicles for the treatment of oncological diseases [9]. According to electron paramagnetic resonance (EPR) data, silicon nanoparticle samples obtained by synthesizing crystalline silicon nanoparticles (nc-Si/ $\text{SiO}_x$ ) via the plasma-chemical method contain  $\sim 10^{18}$  particles/g of paramagnetic centers [10]. Intratumoral administration of sols of iron-doped crystalline silicon (nc-Si/ $\text{SiO}_x$ /Fe) nanoparticles to mice with Lewis lung carcinoma (CLL) reduces tumor cell growth [11]. The authors believe that when nanoparticles dissolve, iron ions are released, resulting in the formation of reactive oxygen species. The MRI method was used to conduct experiments on the observation of nanoparticle accumulation in tumors and tumor growth inhibition. Thus, nc-Si/ $\text{SiO}_x$ /Fe nanoparticles obtained via the plasma-chemical method of synthesis can be used in MRI diagnostics, targeted drug delivery, and oncological disease therapy as thermal sensitizers for hyperthermia. However, for wider nanoparticle applications, the nanoparticles must be colloid stabilized to provide their delivery to tumors in an pristine form. The presence of iron oxides

in the near-surface layer of the nanoparticles was also believed to facilitate their modification by colloidal stability stabilizers.

Numerous experimental and theoretical studies have shown that reducing the size of the investigated particles to the nanometer range causes a qualitative change in the properties of the object. In this case, structural elements can acquire physical, physicochemical, and chemical properties that differ significantly from the properties of a bulk analog. Conversely, the properties of objects with sizes in the order of several nanometers differ from the properties of individual atoms or molecules that compose these objects. This applies to nanoscale crystals and clusters. Therefore, a set of complementary analysis methods are used to obtain information on the structural and physical properties of nanoparticles [12, 13].

This work aimed to study the properties of iron-containing silicon nanoparticles using a variety of analytical methods, as well as their colloidal stabilization with citrate anions for theranostic applications, e.g., as MRI contrast agents.

## MATERIALS AND METHODS

We used iron-containing nanocrystalline silicon (*GNIKhTEOS*, Russia) obtained using the plasma-chemical method [12], deionized water from a Milli-Q water purification unit with a specific conductivity of 18  $\mu\text{S}/\text{cm}$ , trisodium citric acid dihydrate (*Helicon*, Russia), and a pH 7.4 phosphate salt buffer solution (*Helicon*) for the modification.

We used K562 erythroleukemia cells (*BioloT*, Russia), a Rosewell Park Memorial Institute medium (*PanEco*, Russia) containing 10% fetal bovine serum (FBS) (BIOSERA, France), 100 U/mL penicillin, and 100  $\mu\text{g}/\text{mL}$  streptomycin (*PanEco*) to assess cytotoxicity. A solution of 3-[4,5-dimethylthiazol-2-yl] 2,5-diphenyltetrazolium bromide (MTT) (*Sigma-Aldrich*, USA) in a phosphate buffer solution with a concentration of 5  $\text{mg}/\text{mL}$  was used for the MTT test. The viability of the nanoparticle-treated cells was measured on a plate spectrophotometer after the cell lines were grown in a  $\text{CO}_2$  incubator.

**Plasmochemical synthesis of nc-Si/SiO<sub>x</sub>.** The plasma-chemical method was used to produce nanosilicon. The synthesis was carried out in a closed-cycle gas system. The system was filled with a highly purified inert gas (Ar, HP, 99.998%) from the line [12]. A plasma evaporator–condenser operating in a low-frequency arc discharge was used as a reactor. A gas flow from an appropriate metering device was used to feed the initial raw material, silicon powder (99.99%), into the reactor. The reactor was fed

with elemental iron (from 2.5 to 10 at %), and at a temperature of  $\sim 10000^\circ\text{C}$ , the powder evaporated in the reactor.

**Elemental composition analysis.** Laser spark emission spectroscopy was used to determine the following main impurity elements in silicon nanoparticles obtained without the addition of iron [12]: Fe, Cu, W, Ca, Mg, Al, Ni, Pb, Ti, Zr, Zn, Sn, Cr, P, and Mo (arranged in decreasing order of the intensity of the analytical signal). The analysis was carried out after a tablet was formed from the powder sample. The total impurity element content in the investigated samples did not exceed 0.8%. Elemental analysis was performed independently using atomic emission spectroscopy with an excitation of the spectrum in an alternating current arc. The following main impurity elements were determined in the obtained nanosilicon samples: Mg (0.03%), Al (0.02%), Ca (0.002%), Fe (0.006%), Ni (0.002%), and Cu (0.019%). Thus, the total content of impurity elements W, Pb, Ti, Zr, Zn, Sn, Cr, P, and Mo did not exceed  $\sim 0.6\%$ .

**Fourier-transform infrared (FTIR) Spectroscopy.** We used a Nicolet iS5 infrared Fourier spectrometer (*Thermo Scientific*, USA) with an iD1 attachment and a resolution of 4  $\text{cm}^{-1}$  (32 scans each for each sample) in the transmission mode and in the wavenumber range of 4000–400  $\text{cm}^{-1}$  to measure the absorption spectra of the nc-Si/SiO<sub>x</sub> samples and an aerosol sample (SiO<sub>2</sub> powder) with a particle size of about 15 nm. The samples were pre-compressed into tablets using potassium bromide (KBr) as an optically transparent matrix (0.30 mg of the sample per 100 mg KBr).

**Sample analysis by X-ray photoelectron spectroscopy (XPS).** The electronic structure and valence states of the obtained nc-Si/SiO<sub>x</sub>/Fe samples were analyzed by XPS using an ESCALAB MK2 electronic spectrometer (*VG Scientific*, Great Britain) with an X-ray source  $\text{MgK}_\alpha$  ( $h\nu = 1253.6$  eV). A nanoparticle powder sample was applied to a conductive vacuum tape, and the total area of the sample was analyzed (about 1  $\text{cm}^2$ ). Survey spectra had a transmission energy of  $-50$  eV, while individual lines of elements had a transmission energy of 20 eV. The accumulation time per point was 0.3 s per 1 pass. The binding energies for the element spectra ranged from  $\pm 10$  to 15 eV relative to the position of the peak maximum. The measurement steps were 0.1 eV for the spectra of the individual lines of elements and 0.25 eV for the survey spectra. The pressure in the analysis chamber of the spectrometer was up to  $5 \cdot 10^{-7}$  Pa.

The charge of the samples was corrected using the standard binding energy (285.0 eV) of the C 1s line of carbon contained in the adhesive tape. The valence states of the elements in the samples were determined

from the chemical shift and the shape (width) of the lines. For elemental and chemical analysis of the samples, Si 2p, C 1s, O 1s, and Fe 2p analytical lines were used, which were measured separately and in the form of an overview spectrum [14].

**Preparation of the nc-Si/SiO<sub>x</sub>/Fe colloidal solution.** To obtain an aqueous colloidal solution of nc-Si/SiO<sub>x</sub>/FeO<sub>x</sub> nanoparticles, 20 mg of the particles was suspended in 10 mL of water. The resulting suspension was dispersed for 5 min using an INLAB ultrasonic generator (16–25 kHz frequency, power no less than 630 W). The samples were centrifuged for 2 min at a rotation speed of 5000 rpm, and the supernatant was collected and passed through a filter with a pore diameter of 0.45 μm (CHROMAFIL AO-45/25 MN). The final particle concentration was 0.14 mg/mL, as determined gravimetrically.

**Modification of the nc-Si/SiO<sub>x</sub>/FeO<sub>x</sub> nanoparticles with citrate ions.** For modification, 20 mg of nc-Si/SiO<sub>x</sub>/Fe nanoparticles was suspended in a solution of citric acid trisodium salt dihydrate (1%, 2%, and 5%) and subsequently dispersed for 5 min in an ultrasonic bath using a QSONICA SONICATORS ultrasonic generator (USA) (frequency 20 kHz, power 125 W). The mixture was stirred in a magnetic stirrer for 24 h at a stirring rate of 600 rpm and centrifuged for 2 min at a rotation rate of 5000 rpm. The supernatant was collected and passed through a filter with a pore diameter of 0.45 μm (CHROMAFIL AO-45/25 MN). Thereafter, the prepared solutions were dialyzed against water for 24 h in a dialysis bag. The final particle concentration was 0.6 mg/mL, as determined gravimetrically.

**The particle hydrodynamic diameter** was evaluated using a zeta potential and molecular weight 90Plus Particle Size Analyzer (*Brookhaven Instruments Corporation*, USA). The measured particle sizes ranged from 4 nm to 6 μm. The measurements were recorded at a temperature of 25°C and a fixed laser scattering angle of 90° at 661 nm. The dispersion medium was deionized water from a Milli-Q water purification unit with a specific conductivity of 18 μS/cm.

**The zeta potential** of the obtained particles was evaluated using a zeta potential and molecular weight 90Plus Partical Size Analyzer with an additional device called Zeta-PALS, which has a sensitivity that allows it to detect the zeta potential three orders of magnitude more accurately than traditional light scattering methods.

**Analysis of nanosilicon cytotoxicity.** A standard colorimetric MTT test, which allows for the quantitative determination of viable cells using a Multiskan Ascent plate reader (*Thermo Fisher Scientific*, USA), was used

to investigate the toxicity of silicon nanoparticles. The K562 erythroleukemia cells in a volume of 100 μL were seeded in a 96-well plate. The initial suspension of the nanosilicon particles was diluted in a physiological solution with phosphate-buffered saline in a ratio of 1:100, resulting in a concentration of 730 μg/mL, and thereafter, it was sonicated. Next, a series of 5-fold dilutions was prepared from the first dilution of 1:100. For each point, 5 μL of the obtained diluted suspensions was added to the cells four times. Four wells with cells that had not been treated with any compound (control wells) remained. The plate was placed in a CO<sub>2</sub> incubator. After 48 h, 5 μL of the MTT reagent solution was added to all wells, and the plate was placed in a CO<sub>2</sub> incubator for 3 h. After incubation, 100 μL of lysis buffer was added to all the wells, and the plate was sealed in a bag and left overnight at room temperature to allow cell lysis and dissolution of the formed formazan crystals. The next day, absorbance was measured at 540 nm (formazan) and 690 nm (background) using a plate spectrophotometer. For each well with cells, the optical density (OD) of formazan, which is proportional to the number of cells in the well, was calculated:

$$\text{OD (well with cells)} = (\text{OD}_{540} - \text{OD}_{690}) \times \\ \times (\text{well with cells}) - \text{average} (\text{OD}_{540} - \text{OD}_{690}) \times \\ \times (\text{wells without cells}).$$

Next, the average of the four repetitions at each point was calculated. The average OD values for the points where compounds were added were divided by the average OD value for the point where no compound was added, which was set as 1, to obtain the proportion of surviving cells relative to the control (untreated) cell.

## RESULTS AND DISCUSSION

In this study, we used nc-Si/SiO<sub>x</sub>/Fe nanoparticles obtained from silicon powder (sample No. 1) using the plasma-chemical method. According to the laser spark emission spectroscopy and XPS results, the resulting particles contain iron (about 0.2 at %). Arc laser ablation of iron ions from the surface of metal electrodes may have occurred during synthesis. According to the EPR data, nc-Si/SiO<sub>x</sub>/Fe contains about ~10<sup>18</sup> particles/g of paramagnetic centers [10]. To increase magnetic susceptibility, the nanoparticles were enriched with iron during the synthesis. During loading, elemental iron with different Fe/Si atomic ratios (from 2.5 to 10 at %, samples 2–7) was added to the feedstock. Immediately after the synthesis, the dispersion of the powder in different batches of material was controlled by measuring nitrogen adsorption isotherms at 77 K using the Brunauer–Emmett–Teller (BET) method [12]. Samples were obtained with different specific surface

areas ranging from 28 to 57 m<sup>2</sup>/g, which correspond to the average particle size  $D_{\text{BET}}$  ranging from 45 to 92 nm when converted to the diameter of an equivalent sphere (Table 1).

To diagnose and predict the properties of a nanomaterial, detailed information about its structural and morphological properties is required. Therefore, a detailed analysis of the particle structure of the obtained material was conducted before its practical application.

**Analysis of the FTIR spectrum of the silicon nanoparticles.** FTIR spectroscopy can be used to obtain information on the composition of the shell of silicon nanocrystals, the state of their surface, and the dynamics of their possible degradation.

The FTIR spectrum of the No. 1 nc-Si/SiO<sub>x</sub>/Fe sample (Fig. 1a) was compared with that of the aerosil sample (SiO<sub>2</sub> powder) with a particle size of about 15 nm (Fig. 1b). Intense absorption bands were found in the FTIR spectrum of the nanosilicon particle sample obtained via plasma-chemical synthesis, indicating the formation of an oxide shell (461, 799, and 1097 cm<sup>-1</sup> SiO<sub>2</sub> or SiO<sub>x</sub>, 0 ≤ x ≤ 2) [12]. The low-intensity absorption peak corresponding to the vibration of the Fe–O bond (580 cm<sup>-1</sup>) [11] indicates the presence of iron oxide in the near-surface layer of the nanoparticle.

**XPS data analysis.** We used previously reported data [15–17] to interpret the results obtained on the possible oxide states of silicon in the investigated samples. According to these data, the binding energy of the Si<sup>0</sup> 2p<sub>3/2</sub> line is 99.8 eV [14, 18, 19], and the chemical shifts of the oxide forms of Si<sub>x</sub><sup>+</sup> relative to Si<sup>0</sup> are 0.9–1.0 eV (Si<sup>1+</sup>), 1.7–1.85 eV (Si<sup>2+</sup>), 2.5–2.6 eV (Si<sup>3+</sup>),

and 3.5–3.7 eV (Si<sup>4+</sup>). According to Crist [16], the peak widths at half maximum for Si 2p and various silicon oxide forms are 1.0 eV (Si<sup>0</sup>), 1.8 eV (Si<sup>1+</sup>), 1.9 eV (Si<sup>2+</sup>), 2.1 eV (Si<sup>3+</sup>), and 1.4–1.5 eV (Si<sup>4+</sup>).

The spectra of the Si 2p line were decomposed using the technique proposed in a previous report [20]. The nonlinear background of secondary electrons was subtracted using the Shirley method [21]. For each oxidation state of silicon, a Si 2p spin doublet (Si 2p<sub>3/2</sub> and Si 2p<sub>1/2</sub>) with a spin-orbit splitting of 0.61 eV and an area ratio of 2:1 was specified. For different oxidation states of silicon, the binding energies and the abovementioned peak widths at half maximum were set [16, 17].

The spectra of the Si 2p line were decomposed on the assumption that silicon was present on the surface of the analyzed particles only in the form of elemental silicon and oxygen-containing compounds, except for the formation of silicon carbide and the presence of residual hydride (SiH<sub>4</sub>) or iron silicide (FeSi, FeSi<sub>2</sub>), which are indistinguishable from Si<sup>1+</sup> in terms of chemical shift and Si<sup>0</sup> and are present in small amounts.

The binding energies of Si 2p<sub>3/2</sub>, O 1s, C 1s, and Fe 2p<sub>3/2</sub> were 99.6, 532.8, 285.0, and 706.7 eV, respectively [16, 17]. In the case of sample charging and line broadening, the possible peak widths at half maximum in the decomposition of the spectra for various forms of silicon and carbon were set in the form of intervals, monotonically increasing as the oxidation state of silicon increased. For the iron line, the spectra had a more complex shape due to a large number of valence electrons, but they were set similarly, with a shift relative to the standard position.

**Table 1.** Characteristics of the nc-Si/SiO<sub>x</sub>/Fe samples

Sample	1	2	3	4	5	6	7
Iron content in raw materials, at %	0	2.5	2.5	5.0	5.0	10.0	10.0
Specific surface, m <sup>2</sup> /g	57.0	28.0	57.0	31.6	48.1	41.6	48.3
Average particle diameter, $D_{\text{BET}}$ , nm	45.2	91.9	45.2	81.5	53.5	61.0	53.3
Si* content, at %	34.1 ± 1.7	20.6 ± 1.0	9.5 ± 0.5	36.5 ± 1.8	35.9 ± 1.8	61.6 ± 3.1	32.1 ± 1.6
Fe* content, at %	0.2	0.5	0.4	0.4	0.5	2.2	0.8
Atomic ratio Fe/Si, %	0.6	2.5	4.0	1.1	1.5	3.5	2.6

\*Element content in near-surface nc-Si/SiO<sub>x</sub>/Fe layers according to the XPS data (scanning depth up to 5 nm).

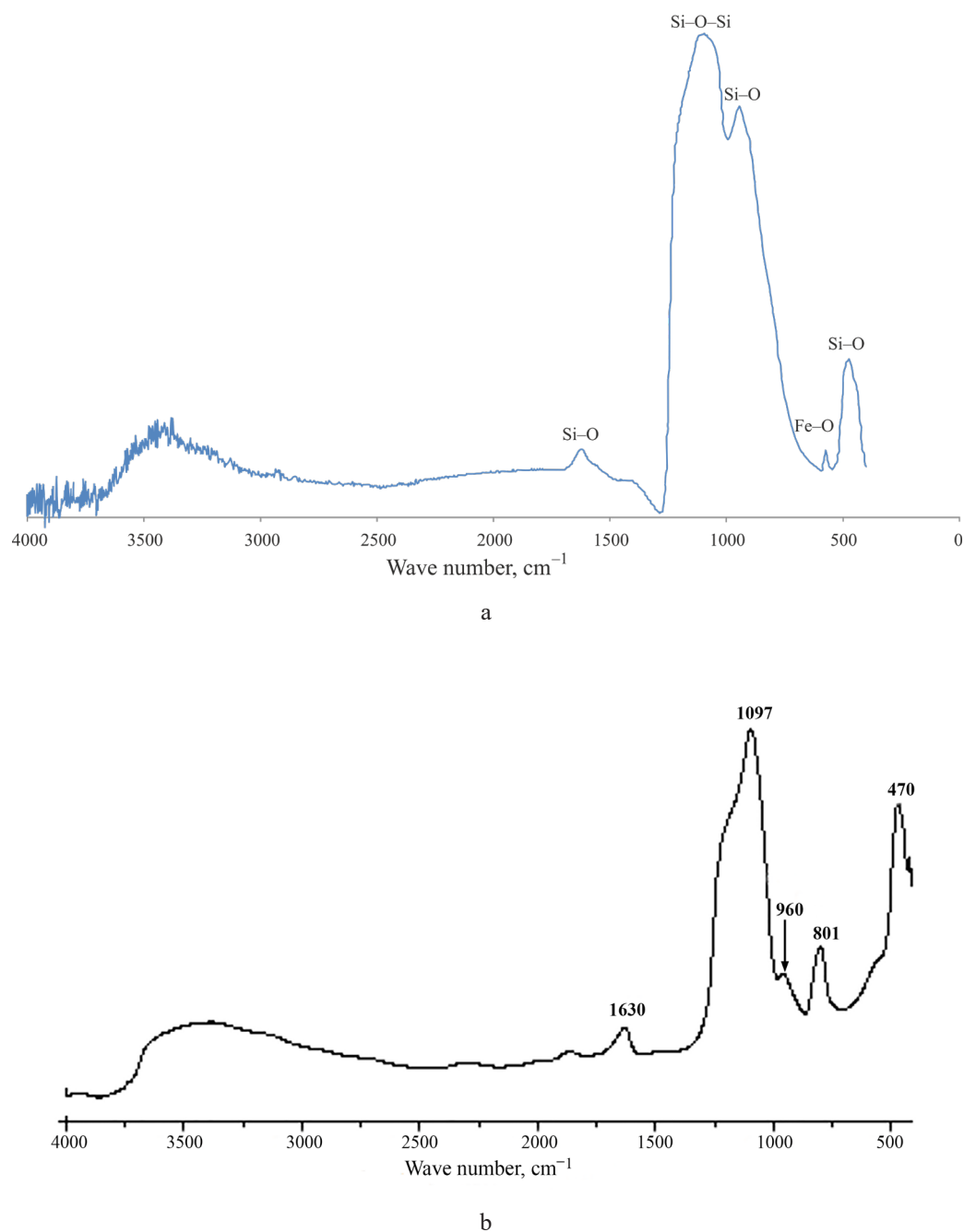


**Fig. 1.** FTIR spectrum of (a) the studied nc-Si/SiO<sub>2</sub>/Fe sample (0.3 mass % in KBr) and (b) the aerosil sample (powdered SiO<sub>2</sub> with a particle size of 15 nm).

Table 1 shows a summary of the measurement results. The particle composition was assumed to be average and constant up to the depth of selection of analytical information in the calculations, with components in the order of 5 nm for silicon and silicon dioxide.

The following conclusions can be drawn from the calculated atomic percentages. Sample 6 mainly contains silicon dioxide on the surface. Samples 2, 3, 4, and 7 have a very similar distribution of silicon oxide forms. The significant difference in the silicon content in the different samples can be explained

by the peculiarities of sample preparation for XPS and the ability of the nanosilicon surface to adsorb various impurities.

The difference between the diminished iron content and the estimated one based on the initial load can be explained as follows. Since the process of mixing iron with the silicon starting material occurs at elevated temperatures, iron oxide particles melt and become covered with silicon, which oxidizes into silicon dioxide during oxidation, significantly reducing the signal from iron (exponential decay of the photoelectron intensity due to the coating layer).

This could also explain why silicon is predominantly present in the form of dioxide. Thus, samples in which the iron content is proportional to the iron content in the feedstock or slightly exceeds its value (measurement and processing error) have a large specific surface area and small particle size, and therefore, silicon (or its dioxide) does not cover iron oxide particles to the same extent as in samples with a relatively small specific surface.

Based on the obtained data, the particle can be assumed to have a silicon core with an amorphous oxide shell, which is silicon oxide with different oxidation states  $\text{SiO}_x$  ( $0 \leq x \leq 2$ ). This is consistent with the data obtained in a previous study [10] based on the analysis of transmission electron images, microscope images, and radiographs. X-ray diffraction studies [11] revealed that the oxidation of the surface of silicon particles resulted in the formation of particles with a “core-shell” structure, which has a silicon nanocrystal as the core and silicon oxides of various oxidation states in the shell. The degree of crystallinity of the sample is  $\sim 10\%$  for the amorphous shell and  $\sim 42\%$  for the crystalline core [11].

For modification with citrate anions, we used an nc-Si/SiO<sub>x</sub>/Fe sample (No. 5) with a diameter of about 48.1 nm and an iron content of about 0.5 at %.

#### Modification of nc-Si/SiO<sub>x</sub>/Fe nanoparticles with citrate anions

Crystalline silicon nanoparticles doped with iron oxide are hydrophilic and form a colloidal solution in aqueous media. However, even freshly prepared nc-Si/SiO<sub>x</sub>/Fe colloidal solutions are unstable. Sols are characterized by a wide particle size distribution. The average particle diameter was about 100 nm, and it increased to 200 nm within a week, then reaching 1000 nm (Table 2). The concentration of the sols changes because of the agglomeration and sedimentation of the particles. The large variation in the zeta potential values of nc-Si/SiO<sub>x</sub>/Fe (from  $-20$  to  $+20$  mV) also indicates the instability of

the colloidal system. An increase in the diameter of silicon nanoparticles results in a change in their physicochemical characteristics [22]. Thus, it is necessary to stabilize silicon nanoparticle sols to use them *in vivo* for theranostics.

To stabilize nc-Si/SiO<sub>x</sub>/Fe, the use of citric acid salt was proposed. Citric acid anions have previously been shown to bind to the surface of hematite ( $\text{Fe}_2\text{O}_3$ ) through chemisorption [23]. The surface of the nc-Si/SiO<sub>x</sub>/Fe particles was shown to be stabilized after being modified with citrate anions. Stable colloidal solutions with a monomodal particle size distribution were formed (Fig. 2). Sols of nc-Si/SiO<sub>x</sub>/Fe-citric nanoparticles modified with citrate anions using a 1% concentration of citric acid trisodium salt dihydrate have a monomodal size distribution with an average diameter of about 60 nm that does not change for a long time (up to 1.5 years). Thus, chemisorption of citrate anions electrostatically stabilizes the interaction forces that determine the tendency of silicon nanoparticles particles to agglomerate.

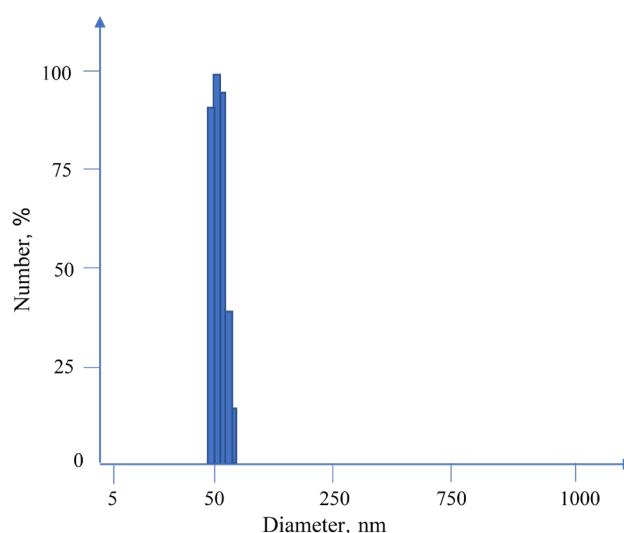


**Fig. 2.** Molecular weight distribution of modified nc-Si/SiO<sub>x</sub>/Fe-citric nanoparticles (1%). The average hydrodynamic diameter was 57 nm.

**Table 2.** Changes in the particle size and aggregation stability of nc-Si/SiO<sub>x</sub>/Fe sols in the original solution and in the solution one week after receiving

Sample	Nanoparticles concentration $C$ , mg/mL	$D_1$ , nm	$D_2$ , nm
nc-Si/SiO <sub>x</sub> /Fe	0.14	112	255–1000
nc-Si/SiO <sub>x</sub> /Fe-citric 1%	0.54	57	64
nc-Si/SiO <sub>x</sub> /Fe-citric 2%	0.70	240	263

Nanoparticles can be modified with citrate anions because of the presence of iron oxides in the near-surface layer of the nanoparticles. An attempt to stabilize iron-free nc-Si/SiO<sub>x</sub>-citric acid nanoparticles obtained by laser CO<sub>2</sub> pyrolysis of silane [24] resulted in their complete precipitation. Therefore, the presence of iron ions in the investigated samples is indirectly confirmed by the formation of stable nc-Si/SiO<sub>x</sub>/Fe-citric colloidal solutions.

#### Cytotoxicity analysis of citrate-modified nanosilicon

The cytotoxicity of citrate-modified nanoparticles was investigated. We used monoclonal K562 human erythroleukemia cell lines for this purpose.

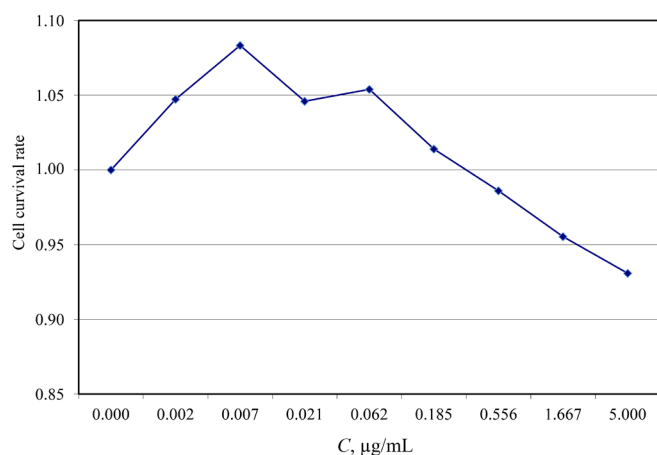


**Fig. 3.** Dependence of the number of surviving cells on the concentration  $C$  of added nc-Si/SiO<sub>x</sub>/Fe-citric nanoparticles after 48 h of exposure.

Figure 3 shows that nc-Si/SiO<sub>x</sub>/Fe-citric nanoparticles do not exhibit cellular toxicity at a concentration of 5 µg/mL. At low concentrations of nc-Si/SiO<sub>x</sub>/Fe-citric nanoparticles, a slight increase in cell proliferation is observed.

## CONCLUSIONS

Iron-containing hybrid silicon nanoparticles were obtained using the plasma-chemical synthesis method. Complementary analytical methods, including laser spark emission spectroscopy, FTIR spectroscopy, X-ray phase analysis, and XPS, were used to analyze the nanoparticles. Based on the obtained data, the nanocrystalline silicon particle can be concluded to have a silicon core covered with a relatively thin layer of intermediate oxides (interface)

and an amorphous oxide shell, which is silicon oxide with different oxidation states SiO<sub>x</sub> ( $0 \leq x \leq 2$ ). The degree of crystallinity of the sample is ~10% for the amorphous shell and ~42% for the crystalline core. According to the XPS data, iron oxides and/or silicides were present in the particle shell in amounts ranging from 0.2 to 2.2 at %, depending on the amount of elemental iron in the starting material. The total content of impurity elements W, Pb, Ti, Zr, Zn, Sn, Cr, P, and Mo did not exceed ~0.6%.

A technique for stabilizing the surface of nanosilicon particles with citrate anions has been developed. It was demonstrated that the presence of iron oxides in the near-surface layer of nanoparticles allows them to be modified with citrate anions, resulting in the formation of stable nc-Si/SiO<sub>x</sub>/Fe colloidal solutions. Since the obtained modified particles are nontoxic, they can be recommended for use in *in vivo* theranostic applications, such as MRI diagnostics.

#### Acknowledgments

The authors are grateful to S.N. Malakhov for carrying out research by the method of IR spectroscopy using the equipment of the resource center "Optics" of the National Research Center "Kurchatov Institute."

#### Authors' contribution

**K.I. Rozhkov** – selection and analysis of literature, Fourier-transform infrared spectroscopy experiment, data processing, discussion of the results, writing the text of the manuscript;

**E.Y. Yagudaeva** – modification of nanoparticles with citrate ions, data processing, discussion of the results, writing the text of the manuscript;

**S.V. Sizova** – data processing, discussion of the results;

**M.A. Lazov** – X-ray photoelectron spectroscopy experiment, data processing, discussion of the results, writing the text of the manuscript;

**E.V. Smirnova** – study of the toxicity of nanoparticles using a standard colorimetric MTT test, data processing, discussion of the results, writing the text of the manuscript;

**V.P. Zubov** – guidance of work on modification of nanoparticles, discussion of the results;

**A.A. Ischenko** – guidance of work on the synthesis of silicon nanoparticles and characterization of their properties, discussion of the results, writing the text of the manuscript.

The authors declare no conflicts of interest.

## REFERENCES

1. Elbeshlawi I., AbdelBaki M.S. Safety of gadolinium administration in children. *Pediatr. Neurol.* 2018;86:27–32. <https://doi.org/10.1016/j.pediatrneurol.2018.07.010>
2. Franckenberg S., Berger F., Schaerli S., Ampanozi G., Thali M. Fatal anaphylactic reaction to intravenous gadobutrol, a gadolinium-based MRI contrast agent. *Radiol. Case Rep.* 2018;13(1):299–301. <https://doi.org/10.1016/j.radcr.2017.09.012>
3. Xu C., Sun S. New forms of superparamagnetic nanoparticles for biomedical applications. *Adv. Drug Deliv. Rev.* 2013;65(5):732–743. <https://doi.org/10.1016/j.addr.2012.10.008>
4. Osminkina L.A., et al. Porous silicon nanoparticles as efficient sensitizers for sonodynamic therapy of cancer. *Micropor. Mesopor. Mater.* 2015;210:169–175. <https://doi.org/10.1016/j.micromeso.2015.02.037>
5. Samira F., Sheikahmadi A. Effect of nanosilicon dioxide on growth performance, egg quality, liver histopathology and concentration of calcium, phosphorus and silicon in egg, liver and bone in laying quails. *Appl. Nanosci.* 2017;7(1–2):765–772. <https://doi.org/10.1007/s13204-017-0620-9>
6. Ksenofontova O.I., Vasin A.V., Egorov V.V., et al. Porous Silicon and Its Application in Biology and Medicine. *Tech. Phys.* 2014;59(1):66–77. <https://doi.org/10.1134/S1063784214010083>
7. Wang L., Jang G., Ban D., et al. Multifunctional stimuli responsive polymer-gated iron and gold-embedded silica nano golf balls: Nanoshuttles for targeted on-demand theranostics. *Bone Res.* 2017;5(1):17051. <https://doi.org/10.1038/boneres.2017.51>
8. Li X., Xia S., Zhou W., Zhan W. Targeted Fe-doped silica nanoparticles as a novel ultrasound–magnetic resonance dual-mode imaging contrast agent for HER2-positive breast cancer. *Int. J. Nanomedicine.* 2019;14:2397–2413. <https://doi.org/10.2147/IJN.S189252>
9. Vaytulevich E.A., Yurmazova T.A., Tuan H.T. Sorbents based on magnetite nanoparticles for biomedical application. *Nanotechnol. Russia.* 2019;14(1–2):33–40. <https://doi.org/10.1134/S1995078019010129>  
[Original Russian Text: Vaytulevich E.A., Yurmazova T.A., Tuan H.T. Sorbents based on magnetite nanoparticles for biomedical application. *Rossiiskie nanotekhnologii.* 2019;14(1–2):31–38 (in Russ.). <https://doi.org/10.21517/1992-7223-2019-1-2-31-38>]
10. Kargina Yu.V., Kharin A.Yu., Zvereva E., et al. Silicon Nanoparticles Prepared by Plasma-Assisted Ablative Synthesis: Physical Properties and Potential Biomedical Applications. *Phys. Status Solidi A.* 2019;216(14):1800897-1–1800897-7. <https://doi.org/10.1002/pssa.201800897>
11. Kargina Yu.V., Zinovyev S.V., Perepukhov A.M., et al. Silicon nanoparticles with iron impurities for multifunctional applications. *Funct. Mater. Lett.* 2020;13(4):2040007-1–2040007-5. <https://doi.org/10.1142/S179360472040007X>
12. Ishchenko A.A., Fetisov G.V., Aslanov L.A. *Nanokremnii: svoistva, poluchenie, primeneniye, metody issledovaniya i kontrolya (Nanosilicon: properties, production, application, research and control methods)*. Moscow: FIZMATLIT; 2012. 648 p. (in Russ.). ISBN 978-5-9221-1369-4
13. Shtikov S.N. (Ed.). *Problemy analiticheskoi khimii. Nanoob"ekty i nanotekhnologii v khimicheskoy analize (Analytical chemistry problems. Nanoobjects and nanotechnology in chemical analysis)*. V. 20. Moscow: Nauka; 2015. 431 p. (in Russ.). ISBN 978-5-02-039185-7

## СПИСОК ЛИТЕРАТУРЫ

1. Elbeshlawi I., AbdelBaki M.S. Safety of gadolinium administration in children. *Pediatr. Neurol.* 2018;86:27–32. <https://doi.org/10.1016/j.pediatrneurol.2018.07.010>
2. Franckenberg S., Berger F., Schaerli S., Ampanozi G., Thali M. Fatal anaphylactic reaction to intravenous gadobutrol, a gadolinium-based MRI contrast agent. *Radiol. Case Rep.* 2018;13(1):299–301. <https://doi.org/10.1016/j.radcr.2017.09.012>
3. Xu C., Sun S. New forms of superparamagnetic nanoparticles for biomedical applications. *Adv. Drug Deliv. Rev.* 2013;65(5):732–743. <https://doi.org/10.1016/j.addr.2012.10.008>
4. Osminkina L.A., et al. Porous silicon nanoparticles as efficient sensitizers for sonodynamic therapy of cancer. *Micropor. Mesopor. Mater.* 2015;210:169–175. <https://doi.org/10.1016/j.micromeso.2015.02.037>
5. Samira F., Sheikahmadi A. Effect of nanosilicon dioxide on growth performance, egg quality, liver histopathology and concentration of calcium, phosphorus and silicon in egg, liver and bone in laying quails. *Appl. Nanosci.* 2017;7(1–2):765–772. <https://doi.org/10.1007/s13204-017-0620-9>
6. Ksenofontova O.I., Vasin A.V., Egorov V.V., et al. Porous Silicon and Its Application in Biology and Medicine. *Tech. Phys.* 2014;59(1):66–77. <https://doi.org/10.1134/S1063784214010083>
7. Wang L., Jang G., Ban D., et al. Multifunctional stimuli responsive polymer-gated iron and gold-embedded silica nano golf balls: Nanoshuttles for targeted on-demand theranostics. *Bone Res.* 2017;5(1):17051. <https://doi.org/10.1038/boneres.2017.51>
8. Li X., Xia S., Zhou W., Zhan W. Targeted Fe-doped silica nanoparticles as a novel ultrasound–magnetic resonance dual-mode imaging contrast agent for HER2-positive breast cancer. *Int. J. Nanomedicine.* 2019;14:2397–2413. <https://doi.org/10.2147/IJN.S189252>
9. Вайтгулевич Е.А., Юрмазова Т.А., Чан Т.Х. Сорбенты на основе наночастиц магнетита для применения в биомедицине. *Российские нанотехнологии.* 2019;14(1–2):31–38. <https://doi.org/10.21517/1992-7223-2019-1-2-31-38>
10. Kargina Yu.V., Kharin A.Yu., Zvereva E., et al. Silicon Nanoparticles Prepared by Plasma-Assisted Ablative Synthesis: Physical Properties and Potential Biomedical Applications. *Phys. Status Solidi A.* 2019;216(14):1800897-1–1800897-7. <https://doi.org/10.1002/pssa.201800897>
11. Kargina Yu.V., Zinovyev S.V., Perepukhov A.M., et al. Silicon nanoparticles with iron impurities for multifunctional applications. *Funct. Mater. Lett.* 2020;13(4):2040007-1–2040007-5. <https://doi.org/10.1142/S179360472040007X>
12. Ищенко А.А., Фетисов Г.В., Асланов Л.А. *Нанокремний: свойства, получение, применение, методы исследования и контроля*. М.: ФИЗМАТЛИТ; 2012. 648 с. ISBN 978-5-9221-1369-4
13. Штыков С.Н. (ред.). *Проблемы аналитической химии*. Т. 20. *Нанообъекты и нанотехнологии в химическом анализе*. М.: Наука; 2015. 431 с. ISBN 978-5-02-039185-7
14. Mosmann T. Rapid colorimetric assay for cellular growth and survival: application to proliferation and cytotoxicity assays. *J. Immunol. Methods.* 1983;65(1–2):55–63. [https://doi.org/10.1016/0022-1759\(83\)90303-4](https://doi.org/10.1016/0022-1759(83)90303-4)
15. Wagner T., Wang J.Y., Hofmann S. Sputter Depth Profiling in AES and XPS. In book: Briggs D., Grant J.T. (Eds.). *Surface Analysis by Auger and X-ray Photoelectron Spectroscopy*. 2003. P. 619–649.

14. Mosmann T. Rapid colorimetric assay for cellular growth and survival: application to proliferation and cytotoxicity assays. *J. Immunol. Methods*. 1983;65(1–2):55–63. [https://doi.org/10.1016/0022-1759\(83\)90303-4](https://doi.org/10.1016/0022-1759(83)90303-4)
15. Wagner T., Wang J.Y., Hofmann S. Sputter Depth Profiling in AES and XPS. In book: Briggs D., Grant J.T. (Eds.). *Surface Analysis by Auger and X-ray Photoelectron Spectroscopy*. 2003. P. 619–649.
16. Naumkin A.V., Kraut-Vass A., Gaarenstroom S.W., Powell C.J. NIST X-ray Photoelectron Spectroscopy Database. NIST Standard Reference Database 20, Version 4.1 (Web Version), 2012. <http://dx.doi.org/10.18434/T4T88K>
17. Crist B.V. Handbook of Monochromatic XPS Spectra: The Elements and Their Native Oxides [Book Review]. *IEEE Electr. Insul. M.* 2003;19(4):73. <https://doi.org/10.1109/MEI.2003.1226740>
18. Gongalsky M.B., Kargina Yu.V., Osminkina L.A., Perepukhov A.M., Gulyaev M.V., Vasiliev A.N., Pirogov Yu A., Maximychev A.V., Timoshenko V.Yu. Porous silicon nanoparticles as biocompatible contrast agents for magnetic resonance imaging. *Appl. Phys. Lett.* 2015;107(23):233702-1-233702-4. <https://doi.org/10.1063/1.4937731>
19. Berridge M.V., Herst P.M., Tan A.S. Tetrazolium dyes as tools in cell biology: new insights into their cellular reduction. *Biotechnol. Annu. Rev.* 2005;11:127–152. [https://doi.org/10.1016/s1387-2656\(05\)11004-7](https://doi.org/10.1016/s1387-2656(05)11004-7)
20. Seah M.P., Spencer S.J. Ultrathin SiO<sub>2</sub> on Si (IV). Intensity measurement in XPS and deduced thickness linearity. *Surf. Interface Anal.* 2003;35(6):515–524. <https://doi.org/10.1002/sia.1565>
21. Vegh J. The Shirley background revised. *J. Electron Spectrosc.* 2006;151(3):159–164. <https://doi.org/10.1016/j.elspec.2005.12.002>
22. Шаронова Н.В., Ягудаева Е.Ю., Сизова С.В. и др. Модификация нанокристаллического кремния полимерами для биомедицинских приложений. *Изв. вузов. Химия и хим. технология*. 2019;62(9):86–96. <https://doi.org/10.6060/ivkkt.20196209.5929>
23. Răcucin M., Creangă D.E., Airinei A. Citric-acid-coated magnetite nanoparticles for biological applications. *Eur. Phys. J. E.* 2006;21(2):117–121. <https://doi.org/10.1140/epje/i2006-10051-y>
24. Dorofeev S.G., Kononov N.N., Ishchenko A.A., et al. Optical and structural properties of thin films precipitated from the sol of silicon nanoparticles. *Semiconductors*. 2009;43(11):1420–1427. <https://doi.org/10.1134/S1063782609110050>
16. Naumkin A.V., Kraut-Vass A., Gaarenstroom S.W., Powell C.J. NIST X-ray Photoelectron Spectroscopy Database. NIST Standard Reference Database 20, Version 4.1 (Web Version), 2012. <http://dx.doi.org/10.18434/T4T88K>
17. Crist B.V. Handbook of Monochromatic XPS Spectra: The Elements and Their Native Oxides [Book Review]. *IEEE Electr. Insul. M.* 2003;19(4):73. <https://doi.org/10.1109/MEI.2003.1226740>
18. Gongalsky M.B., Kargina Yu.V., Osminkina L.A., Perepukhov A.M., Gulyaev M.V., Vasiliev A.N., Pirogov Yu A., Maximychev A.V., Timoshenko V.Yu. Porous silicon nanoparticles as biocompatible contrast agents for magnetic resonance imaging. *Appl. Phys. Lett.* 2015;107(23):233702-1-233702-4. <https://doi.org/10.1063/1.4937731>
19. Berridge M.V., Herst P.M., Tan A.S. Tetrazolium dyes as tools in cell biology: new insights into their cellular reduction. *Biotechnol. Annu. Rev.* 2005;11:127–152. [https://doi.org/10.1016/s1387-2656\(05\)11004-7](https://doi.org/10.1016/s1387-2656(05)11004-7)
20. Seah M.P., Spencer S.J. Ultrathin SiO<sub>2</sub> on Si (IV). Intensity measurement in XPS and deduced thickness linearity. *Surf. Interface Anal.* 2003;35(6):515–524. <https://doi.org/10.1002/sia.1565>
21. Vegh J. The Shirley background revised. *J. Electron Spectrosc.* 2006;151(3):159–164. <https://doi.org/10.1016/j.elspec.2005.12.002>
22. Шаронова Н.В., Ягудаева Е.Ю., Сизова С.В. и др. Модификация нанокристаллического кремния полимерами для биомедицинских приложений. *Изв. вузов. Химия и хим. технология*. 2019;62(9):86–96. <https://doi.org/10.6060/ivkkt.20196209.5929>
23. Răcucin M., Creangă D.E., Airinei A. Citric-acid-coated magnetite nanoparticles for biological applications. *Eur. Phys. J. E.* 2006;21(2):117–121. <https://doi.org/10.1140/epje/i2006-10051-y>
24. Дорофеев С.Г., Кононов Н.Н., Ищенко А.А. и др. Оптические и структурные свойства тонких пленок, осажденных из золя наночастиц кремния. *Физика и техника полупроводников*. 2009;43(11):1460–1467.

#### About the authors:

**Kirill I. Rozhkov**, Postgraduate Student, I.P. Alimarin Department of Analytical Chemistry, M.V. Lomonosov Institute of Fine Chemical Technologies, MIREA – Russian Technological University (86, Vernadskogo pr., Moscow, 119571, Russia). E-mail: rokirill58@mail.ru. <https://orcid.org/0000-0003-4120-837X>

**Elena Y. Yagudaeva**, Cand. Sci. (Chem.), Senior Researcher, M.M. Shemyakin & Yu.A. Ovchinnikov Institute of Bioorganic Chemistry, Russian Academy of Sciences (Miklukho-Maklaya ul., 16/10, Moscow, 117997, Russia). E-mail: elena-yagudaeva@yandex.ru. <https://orcid.org/0000-0001-9782-0811>

**Svetlana V. Sizova**, Cand. Sci. (Chem.), Researcher, M.M. Shemyakin & Yu.A. Ovchinnikov Institute of Bioorganic Chemistry, Russian Academy of Sciences (Miklukho-Maklaya ul., 16/10, Moscow, 117997, Russia). E-mail: sv.sizova@gmail.com. <https://orcid.org/0000-0003-0846-4670>

**Michael A. Lazov**, Assistant, I.P. Alimarin Department of Analytical Chemistry, M.V. Lomonosov Institute of Fine Chemical Technologies, MIREA – Russian Technological University (86, Vernadskogo pr., Moscow 119571, Russia). E-mail: lazovm@gmail.com. <https://orcid.org/0000-0001-8578-1683>

**Evgeniya V. Smirnova**, Cand. Sci. (Biol.), Researcher, M.M. Shemyakin & Yu.A. Ovchinnikov Institute of Bioorganic Chemistry, Russian Academy of Sciences (Miklukho-Maklaya ul., 16/10, Moscow, 117997, Russia). E-mail: smirnova.evgeniya@gmail.com. <https://orcid.org/0000-0002-9744-952X>

**Vitaliy P. Zubov**, Dr. Sci. (Chem.), Professor, S.S. Medvedev Department of Chemistry and Technology of High-Molecular Compounds, M.V. Lomonosov Institute of Fine Chemical Technologies, MIREA – Russian Technological University (86, Vernadskogo pr., Moscow, 119571, Russia). E-mail: zubov@mirea.ru. Principal Researcher, M.M. Shemyakin & Yu.A. Ovchinnikov Institute of Bioorganic Chemistry, Russian Academy of Sciences (Miklukho-Maklaya ul., 16/10, Moscow, 117997, Russia). E-mail: zubov@ibch.ru. <https://orcid.org/0000-0003-3429-0272>

**Anatoliy A. Ischenko**, Dr. Sci. (Chem.), Professor, I.P. Alimarin Department of Analytical Chemistry, M.V. Lomonosov Institute of Fine Chemical Technologies, MIREA – Russian Technological University (86, Vernadskogo pr., Moscow, 119571, Russia). E-mail: aischenko@yasenevo.ru. <https://orcid.org/0000-0003-1532-377X>

#### Об авторах:

**Рожков Кирилл Игоревич**, аспирант кафедры аналитической химии им. И.П. Алимарина Института тонких химических технологий им. М.В. Ломоносова ФГБОУ ВО «МИРЭА – Российский технологический университет» (119571, Россия, Москва, пр-т Вернадского, д. 86). E-mail: rokirill58@mail.ru. <https://orcid.org/0000-0003-4120-837X>

**Ягудаева Елена Юрьевна**, к.х.н., старший научный сотрудник Института биоорганической химии им. акад. М.М. Шемякина и Ю.А. Овчинникова Российской академии наук (117997, Россия, Москва, ул. Миклухо-Маклая, д.16/10). E-mail: elena-yagudaeva@yandex.ru. <https://orcid.org/0000-0001-9782-0811>

**Сизова Светлана Викторовна**, к.х.н., научный сотрудник Института биоорганической химии им. акад. М.М. Шемякина и Ю.А. Овчинникова Российской академии наук (117997, Россия, Москва, ул. Миклухо-Маклая, д.16/10). E-mail: sv.sizova@gmail.com. <https://orcid.org/0000-0003-0846-4670>

**Лазов Михаил Александрович**, ассистент кафедры аналитической химии им. И.П. Алимарина Института тонких химических технологий им. М.В. Ломоносова ФГБОУ ВО «МИРЭА – Российский технологический университет» (119571, Россия, Москва, пр-т Вернадского, д. 86). E-mail: lazovm@gmail.com. <https://orcid.org/0000-0001-8578-1683>

**Смирнова Евгения Владимировна**, к.б.н., научный сотрудник Института биоорганической химии им. акад. М.М. Шемякина и Ю.А. Овчинникова Российской академии наук (117997, Россия, Москва, ул. Миклухо-Маклая, д.16/10). E-mail: smirnova.evgeniya@gmail.com. <https://orcid.org/0000-0002-9744-952X>

**Зубов Виталий Павлович**, д.х.н., профессор, кафедра химии и технологии высокомолекулярных соединений им. С.С. Медведева Института тонких химических технологий им. М.В. Ломоносова ФГБОУ ВО «МИРЭА – Российский технологический университет» (119571, Россия, Москва, пр-т Вернадского, д. 86). E-mail: zubov@mirea.ru. Главный научный сотрудник Института биоорганической химии им. акад. М.М. Шемякина и Ю.А. Овчинникова Российской академии наук (117997, Россия, Москва, ул. Миклухо-Маклая, д.16/10). E-mail: zubov@ibch.ru. <https://orcid.org/0000-0003-3429-0272>

**Ищенко Анатолий Александрович**, д.х.н., профессор, заведующий кафедрой аналитической химии им. И.П. Алимарина Института тонких химических технологий им. М.В. Ломоносова ФГБОУ ВО «МИРЭА – Российский технологический университет» (119571, Россия, Москва, пр-т Вернадского, д. 86). E-mail: aischenko@yasenevo.ru. <https://orcid.org/0000-0003-1532-377X>

*The article was submitted: July 23, 2021; approved after reviewing: September 15, 2021; accepted for publication: October 18, 2021.*

*Translated from Russian into English by H. Moshkov*

*Edited for English language and spelling by Enago, an editing brand of Crimson Interactive Inc.*